

# Quark-gluon vertex and flavour dependence of dynamical chiral symmetry breaking

Fernando E. Serna, Bruno El-Bennich and Chen Chen

Instituto Tecnológico de Aeronáutica, São José dos Campos, SP, Brazil  
Laboratório de Física Teórica e Computacional, Universidade Cruzeiro do Sul, São Paulo, SP, Brazil  
Instituto de Física Teórica, Universidade Estadual Paulista, São Paulo, SP, Brazil



## Introduction

Dynamical chiral symmetry breaking (DCSB) is a remarkably effective mass generating mechanism and is most likely connected with confinement. Indeed, the origin of a constituent quark mass and the fact that DCSB contributes to nearly 98% of visible mass has become a paradigm in contemporary hadron physics. The impact is evident for the light sector and plays an eminent role in describing why three very light current quarks form a nucleon bound state whose mass is about three orders of magnitude larger. For heavier quarks, starting with the strange quark, the effect of DCSB is gradually attenuated and the b-quark's constituent mass is almost completely due to explicit chiral symmetry breaking (CSB) [1, 2]. Somewhere between the strange and charm quark mass the effects of explicit CSB and the sum of explicit and DCSB become more alike. Remarkably, the weak decay constants of light pseudoscalar and vector mesons increase with the light current-quark mass, they level off somewhere between the strange- and charm-quark mass and fall off for heavier quark masses as  $f_M = 1/\sqrt{M}$ . On the other hand, the weak decay constants of radially excited quarkonia can be shown to vanish in the chiral limit but though suppressed, their values strongly increase between the strange and charmed quarkonia [3].

## Gap equation

Since DCSB is a phenomenon emerging from the strong physics of dressed-quarks, it is often studied via QCD's gap equation

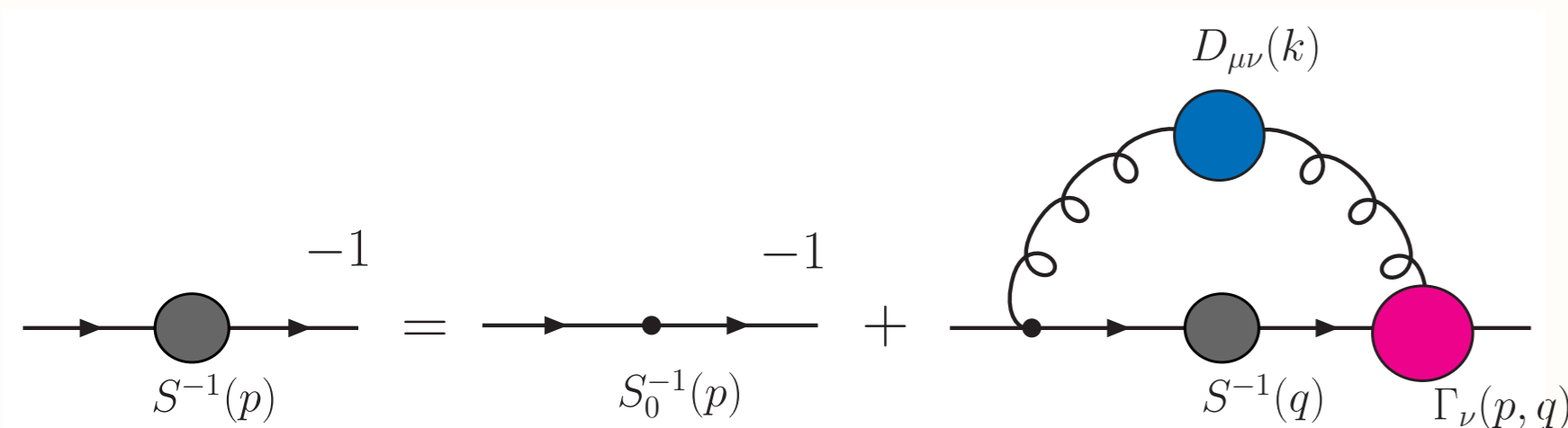


Figure 1: Gap equation

$$S^{-1}(p) = Z_2^f(i\gamma \cdot p + m_f^b) + Z_1^f \int_q^\Lambda g^2 D_{\mu\nu}(p-q) \frac{\lambda^a}{2} \gamma_\mu S(q) \frac{\lambda^a}{2} \Gamma_\nu(p, q)$$

where  $D_{\mu\nu}$  is gluon propagator;  $\Gamma_\nu$  the quark-gluon vertex;  $\Lambda$  the regularization mass-scale;  $m_f^b(\mu, \Lambda)$  the current-quark bare mass, with  $\mu$  being the renormalization point;  $Z_{1,2}(\mu^2, \Lambda^2)$  the vertex and quark wave-function renormalization constants respectively.

## Model Kernels

The quark-DSE kernel is specified by the contraction  $Z_1 g^2 D_{\mu\nu}(p-q) \Gamma_\nu(q, p)$ . Here we compare five kernel models which can be introduced by

$$Z_1 g^2 D_{\mu\nu}(k) \Gamma_\nu(q, p) = k^2 \mathcal{G}(k^2) D_{\mu\nu}^{\text{free}}(k) \Gamma_\nu^A(q, p) = [k^2 \mathcal{G}_{\text{IR}}(k^2) + 4\pi \tilde{\alpha}_{p\text{QCD}}(k^2)] \times D_{\mu\nu}^{\text{free}}(k) \Gamma_\nu^A(q, p)$$

where in all instances we will use

$$4\pi \tilde{\alpha}_{p\text{QCD}}(s) = \frac{8\pi^2 s \gamma_m \mathcal{F}(s)}{\ln[\tau + (1 + s/\Lambda_{\text{QCD}}^2)^2]}$$

with  $\gamma_m = 12/(33 - 2N_f)$ ,  $N_f = 4$ ,  $\Lambda_{\text{QCD}} = 0.234 \text{ GeV}$ ,  $\tau = e^2 - 1$  and  $\mathcal{F}(s) = [1 - \exp(s/4m_t^2)]/s$ ,  $m_t = 0.5 \text{ GeV}$ .

For the infrared, we compare two forms

$$\mathcal{G}_{\text{IR}}^{\text{MT}}(s) = \frac{4\pi^2}{\omega^6} s D e^{-s/\omega^2} \quad \mathcal{G}_{\text{IR}}^{\text{QC}}(s) = \frac{8\pi^2}{\omega^4} D e^{-s/\omega^2}$$

On the other hand,  $\Gamma_\nu^A(q, p)$  is an Ansatz for that part of the dressed quark-gluon vertex, and we employ four models for it:

$$\text{RL}_1 \text{ Ansatz: } \Gamma_\nu^{\text{RL}}(q, p) = \gamma_\nu$$

$$\text{RL}_2 \text{ Ansatz: } \Gamma_\nu^{\text{RL}}(q, p) = Z_2^2 \gamma_\nu$$

$$\text{BC- Ansatz: } \Gamma_\nu^{\text{BC}}(q, p) = f_\Lambda^+(p, q) \gamma_\nu + f_\Lambda^-(p, q) (\not{q} + \not{p})(q + p)_\nu - i f_B^-(p, q) (q + p)_\nu \not{D}$$

$$\text{L+T- Ansatz: } \Gamma_\nu^{\text{L+T}}(q, p) = \Gamma_\nu^{\text{BC}}(q, p) + \Gamma_\nu^{\text{T}}(q, p)$$

where  $\Gamma_\nu^{\text{T}}$  is given by

$$\Gamma_\nu^{\text{T}}(q, p) = \frac{f_\Lambda^-(p, q)}{2} (q - p)^2 \gamma_\nu^{\text{T}} - f_B^-(p, q) \sigma_{\nu\rho} (q - p)_\rho - f_\Lambda^-(p, q) (q_\nu \gamma \cdot p - p_\nu \gamma \cdot q - i \gamma_\nu p_\rho q_\beta \sigma_{\rho\beta})$$

with

$$f_\Lambda^+(p, q) = \frac{\Lambda(q^2) + \Lambda(p^2)}{2}, \quad f_\Lambda^-(p, q) = \frac{\Lambda(q^2) - \Lambda(p^2)}{q^2 - p^2}$$

$$f_B^-(p, q) = \frac{B(q^2) - B(p^2)}{q^2 - p^2}$$

## Quark sigma term

A convenient parameter to study the effect of DCSB is the renormalization-point invariant ratio defined by  $\zeta_f := \sigma_f/M_f^E$ , being  $\sigma_f$  the constituent-quark sigma term, which is defined by

$$\sigma_f = m_f(\mu) \frac{\partial M_f^E}{\partial m_f(\mu)}$$

where  $M_f^E$  is the definition of the Euclidean constituent-quark mass:  $(M_f^E)^2 := \{p^2 | p^2 = M^2(p^2)\}$ .

## Numerical results

In Table. 1, we report the set of parameters that were implemented in our calculations.

Table 1: Set of parameters

Model \ parameters	$(\omega D)^{1/3}$ [GeV]	$\omega$ [GeV]
MT+RL <sub>1</sub>	0.72	0.40
QC+RL <sub>2</sub>	0.80	0.40
MT+BC	0.72	0.50
QC+BC	0.65	0.60
QC+(L+T)	0.80	0.60

We preset in Fig. 2 the quark mass function  $M_f(p^2)$  obtained by solving the quark DSE with the QC+(L+T) Ansatz introduced above.

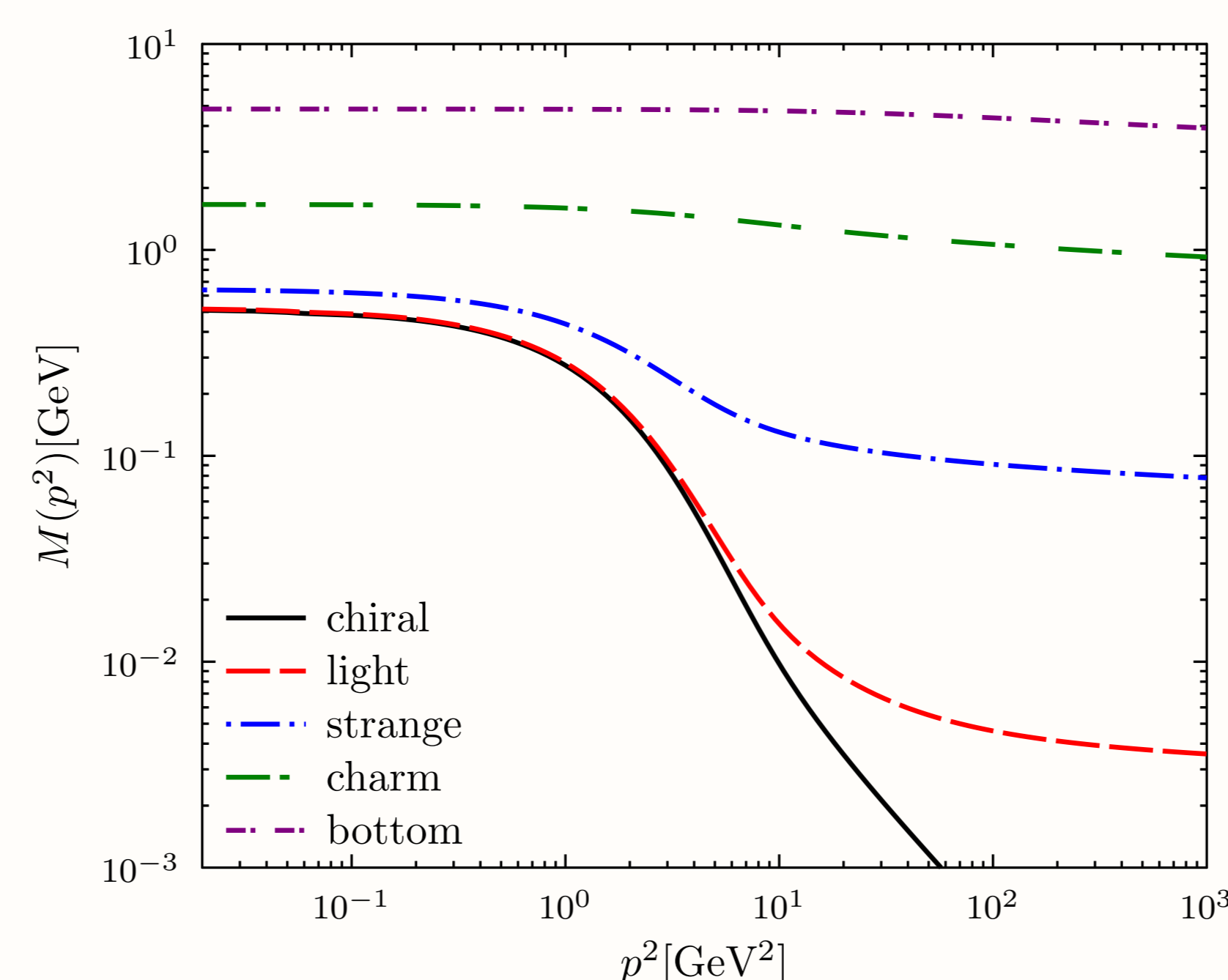


Figure 2:  $M_f(p)$  generated by QC + (L+T) Ansatz.  $M_u(0) = 0.523 \text{ GeV}$ ,  $M_s(0) = 0.645 \text{ GeV}$ ,  $M_c(0) = 1.663 \text{ GeV}$ ,  $M_b(0) = 4.832 \text{ GeV}$ .

In Tables. 2 and 3 we report respectively the results obtained for the Euclidean constituent quark masses  $M_f^E$  and the renormalization point invariant  $\zeta_f$  for the different models studied here.

Table 2: Euclidean quark masses  $M_f^E$  (GeV)

f	u, d	s	c	b
$m_f(\mu)$	0.0037	0.082	0.970	4.100
$(M_f^E)^{\text{MT+RL}_1}$	0.403	0.555	1.566	4.682
$(M_f^E)^{\text{QC+RL}_2}$	0.471	0.622	1.630	4.722
$(M_f^E)^{\text{MT+BC}}$	0.477	0.582	1.548	4.666
$(M_f^E)^{\text{QC+BC}}$	0.281	0.403	1.235	4.081
$(M_f^E)^{\text{QC+(L+T)}}$	0.459	0.566	1.526	4.648

Table 3: Renormalization-point invariant ratio  $\zeta_f$ .

f	u, d	s	c	b
$\zeta_f^{\text{MT+RL}_1}$	0.025	0.234	0.642	0.851
$\zeta_f^{\text{QC+RL}_2}$	0.021	0.208	0.614	0.825
$\zeta_f^{\text{MT+BC}}$	0.013	0.172	0.653	0.853
$\zeta_f^{\text{QC+BC}}$	0.036	0.248	0.701	0.918
$\zeta_f^{\text{QC+(L+T)}}$	0.011	0.185	0.659	0.852

In Fig. 3 we depicted the evolution of  $\zeta_f$  as function of the bare quark mass for the case of each model investigated in this work.

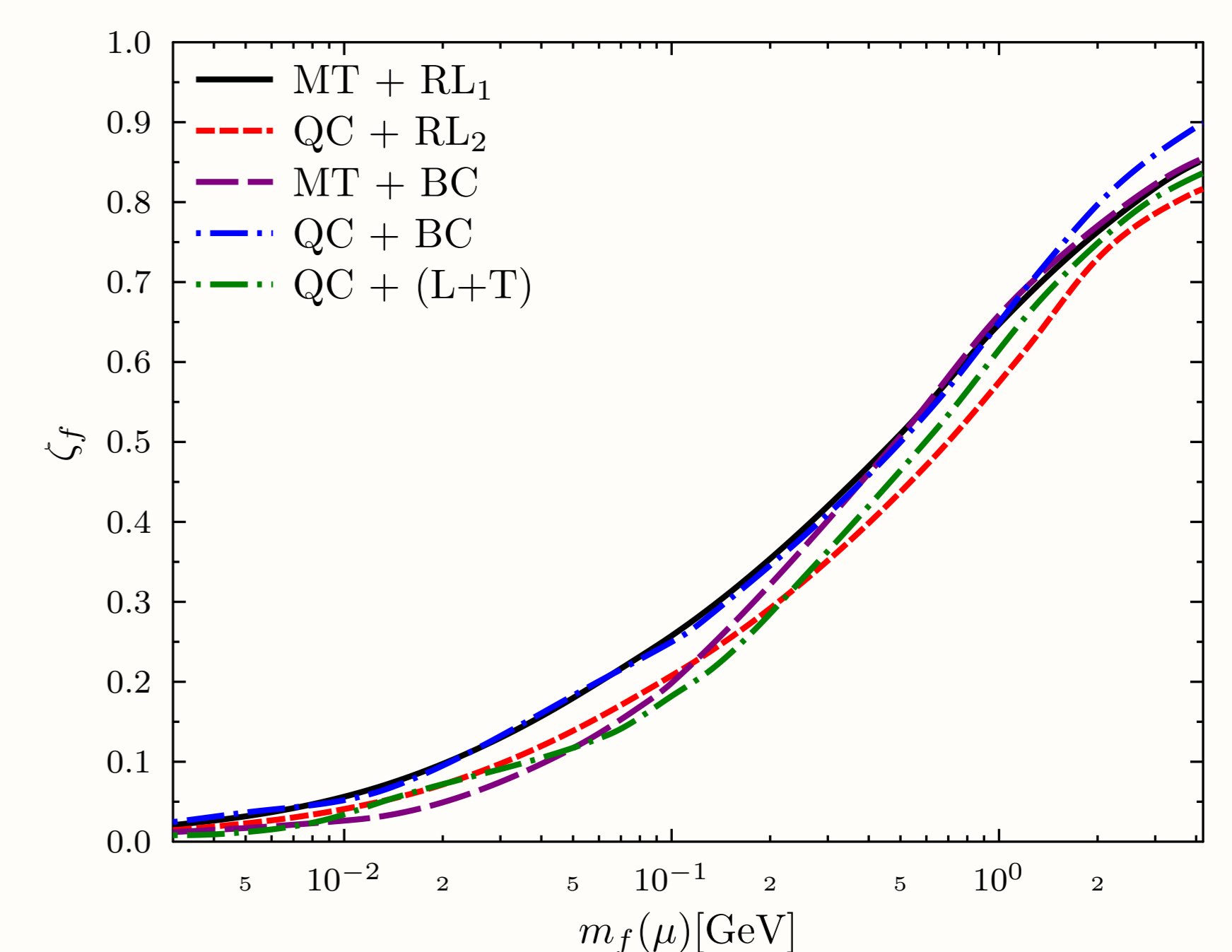


Figure 3:  $\zeta_f$  as a function of  $m_f(\mu)$ .

## Final Remarks

In this work, we have investigated at which mass scale these effects of CSB and DCSB are comparable in dependence of:

- A chosen gluon interaction model
- An ansatz for the quark-gluon vertex

As we have seen, this occurs somewhere midway between the strange and charm mass and is fairly independent of the ingredients in the quark-gap equation.

## Acknowledgements

Work partially financed by CNPq Grant No. 168240/2017-3 (F.E.S), FAPESP Grants No. 2016/03154-7 (B.E.-B) and 2015/21550-4 (C.C).

## References

- [1] A. Höll, P. Maris, C. D. Roberts and S. V. Wright, Nucl. Phys. Proc. Suppl. 161, 87 (2006).
- [2] B. El-Bennich, Craig D. Roberts and Mikhail A. Ivanov, PoS QCD-TNT-II 018 (2012).
- [3] B. El-Bennich, EPJ Web Conf. 172, 02005 (2018).